Photodiagnosis and Photodynamic Therapy 27 (2019) 375–379

Contents lists available at ScienceDirect

Photodiagnosis and Photodynamic Therapy

journal homepage: www.elsevier.com/locate/pdpdt

Optical screening of hepatitis-B infected blood sera using optical technique and neural network classifier

Saranjam Khan[a,*], Rahat Ullah[b], Ruby Ashraf[c], Ajmal Khan[c], Shamim Khan[a], Iftikhar Ahmad[d]

[a] Department of Physics, Islamia College Peshawar, Khyber Pakhtunkhwa, Pakistan
[b] Agri-Biophotonics Division, National Institute for Lasers and Optronics, Nilore, Islamabad 45650, Pakistan
[c] Department of Chemistry, COMSATS Institute of Information Technology, Abbottabad, 22060, KPK, Pakistan
[d] Institute of Radiotherapy and Nuclear Medicine (IRNUM), University Campus, Peshawar, Pakistan

ARTICLE INFO

Keywords:
Hepatitis B (HBV)
Raman spectroscopy
Nueral Network classifier

ABSTRACT

In this study we demonstrate the analysis of biochemical changes in the human blood sera infected with Hepatitis B virus (HBV) using Raman spectroscopy. In total, 120 diseased blood samples and 170 healthy blood samples, collected from Pakistan Atomic Energy Commission (PAEC) general hospital, were analyzed. Spectra from each sample of both groups were collected in the spectral range 400-1700 cm^{-1}. Careful spectral analyses demonstrated significant spectral variations ($p < 0.0001$) in the HBV infected individuals as compared to the normal ones. The spectral variations presumably occur because of the variations in the concentration of important biomolecules. Variations in spectral signatures were further exploited by using a neural network classifier towards machine-assisted classification of the two groups. Evaluation metrics of the classifier showed the diagnostic accuracy of (0.993), sensitivity (= 0.992), specificity (= 0.994), positive predictive value (= 0.992) and negative predictive value (= 0.994). The observed variations in the molecular concentration may be important markers of the hepatic performance and can be used in the diagnosis and machine-assisted classification of HBV infection.

1. Introduction

Hepatitis B (HB) is a primary health problem affecting millions of individuals internationally each year. Specifically, as per the estimates of the World Health Organization (WHO), the global annual rate of chronic HB-infection and related deaths are approximatly 240–250 million and 780,000, respectively. In chronic HB infection, the virus remains active inside the body of an infected individual, posing a potential health risk not only to the individual but also to the community. Specifically, the infection/virus can transmit from the infected to healthy individuals via body fluids. Moreover, it has been observed that there is more likelihood (90%) of developing a chronic infection in the young adult [1]. It is unfortunate that Pakistan is among the worst HB affected nation with about 9 million HBV infected patients [2].

The HB virus (HBV) consists of double-stranded DNA; the core of the virus comprises of DNA and DNA polymerase surrounded by an outer layer of various proteins referred as hepatitis B surface proteins (HBsAg). The HBsAg is detectable in the blood serum after the infection, even before the appearance of the symptoms. The presence of HBsAg in the bloodstream is considered as the gold standard for the disease presence whereas HBsAg for over six months is the indicator of chronic infection [3–5]. An accurate and timely diagnosis of the disease is critical for the proper management and better clinical outcomes of the disease. Different types of chemical diagnostics tests performed in general for the detection of HBV infection, include Polymerase Chain Reaction (PCR) and Enzyme-Linked Immunosorbent Assay (ELISA). PCR is used for the HB DNA and DNA polymerase soon (one week) after the infection to HB virus. However, the PCR is not recommended in routine at mass scale as it is effective only in the first week of the infection. Moreover, PCR is time consuming and expensive procedure. In contrast, ELISA, which detects HBsAg in the blood serum, is a standard test for the diagnosis of HBV; the primary shortcoming associated with ELISA is the limited sensitivity at the early stage of the infection, which, in turn, has been correlated to the delayed production of HBsAg. In addition, the clinical use of ELISA is sometimes compromised by the high rate of false positive and false negative results [6]. Because of these limitations, there is a pressing need for a cost-effective, fast and simple laboratory test that diagnose the infection at an early stage.

Recently, Raman spectroscopy (RS) has gained widespread interest in biomedical diagnosis [7,8]. RS is basically an inelastic scattering of

* Corresponding author.
E-mail addresses: k.saranjam@yahoo.com (S. Khan), iahmadmp@gmail.com (I. Ahmad).

https://doi.org/10.1016/j.pdpdt.2019.07.001
Received 22 May 2019; Received in revised form 27 June 2019; Accepted 8 July 2019
Available online 09 July 2019

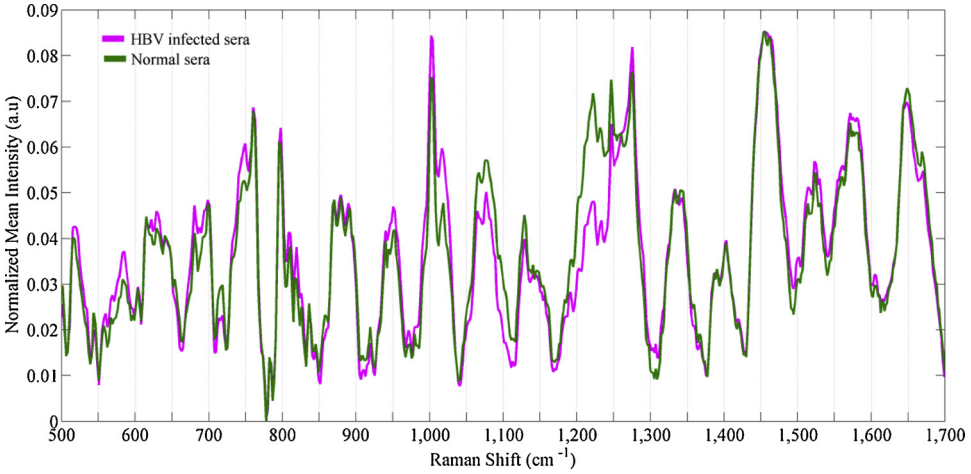

Fig. 1. Normalized Mean Raman spectra from healthy (green) and Hepatitis B (magenta) human blood sera samples.

Table 1
Summary of the peak position, peak values, *p*-values and confidence intervals for the Raman spectra of normal and HBV samples.

Sr. No.	Peak Position	Peak Value		*p* value (95% Confidence Interval)
		Normal	HBV	
1	520	0.245	0.213	< 0.0001(0.03 -0.04)
2	640	0.232	0.276	< 0.0001(−0.06 to −0.03)
3	680	0.467	0.569	< 0.0001(−0.11 to −0.08)
4	747	0.673	0.753	< 0.0001(−0.08 to −0.06)
5	765	0.497	0.592	< 0.0001(−0.09 to −0.07)
6	790	0.746	0.823	< 0.0001(−0.08 to −0.05)
7	830	0.436	0.384	< 0.0001(0.04 -0.07)
8	910	0.211	0.087	< 0.0001(0.11 - 0.14)
9	960	0.365	0.243	< 0.0001(0.11 - 0.13)
10	1005	0.038	0.042	0.042(−0.02 to −0.01)
11	1025	0.339	0.399	< 0.0001(−0.07 to −0.05)
12	1125	0.362	0.514	< 0.0001(−0.16 to −0.14)
13	1222	0.674	0.732	< 0.0001(−0.06 to −0.04)
14	1275	0.515	0.337	< 0.0001(0.16 - 0.19)
15	1403	0.660	0.568	< 0.0001(0.08 - 0.09)
16	1470	0.976	0.999	0.072(−0.02 - 0.00)
17	1500	0.452	0.352	< 0.0001(0.09 - 0.11)
18	1580	0.638	0.665	< 0.0001(−0.03 to −0.01)

incident light photon as result of interaction with the (biological) sample. Consequently upon the interaction with intramolecular bonds of the sample, the energy of the incident photon is partially transferred, raising the molecules to excited vibrational states. During the relaxation process, the photon scatters with a different energy. This difference in energy, termed as Raman shift, provides molecular specific information of the target sample. Specifically, each biomolecule has a characteristics Raman shift. The peak positions of Raman spectra provide information about the composition, whereas the peak intensity shows the concentration of the particular molecule in the sample. In diseases like cancer and infections, the anomaly starts at the molecular level- typically undetected with the normal chemical tests; nevertheless, Raman spectroscopy has the capability to assess and observe these variations in the molecular composition [9–11].

Unlike the conventional diagnostic tests, Raman spectroscopy has many attractive features but still has some limitations as well. Variations in spectral signatures between normal and pathological samples is normally very minimal that can not perceived with naked eye. So for the applications of Raman spectroscopy as diagnostic techniques there is rigorous need for computer algorithm that divided the given data into different classes on the basis of available information. The model capture the useful information from the data set and categorize them accordingly. The most commonly used classification algorithm include PCA [12] and support vector machine (SVM) [13,14], PLS [15] and LDA [16].

In the current study, the contrast in the Raman spectra of normal and pathological sera samples in tandem with machine assisted classification has been presented. In particular, Raman spectroscopy was exploited to investigate the biomolecular changes in the sera of HBV infected patients and healthy controls. The observed spectral differences were used to train and validate neural network classifier towards machine assisted discrimination of the two groups. Evaluation metrics of the classification algorithm showed the promise of the presented technique for clinical implementation in the future.

2. Material and Methods

2.1. Sample collection and preparation

In total of 120 HBV infected samples, collected from PAEC General Hospital Islamabad, Pakistan were used. A prior approval has been obtained from the ethical committee of PAEC General Hospital Islamabad, Pakistan before sample collection. These samples were confirmed HBV^+ on the basis of ELISA findings. For comparison, 170 blood samples from healthy volunteers of the same age group and different gender having a normal medical history were used. All these samples were acquired in EDTA tubes containing a clot activator gel (HebeiXinle, Sci&Tech Co. Ltd., China). Sera were then extracted from all these blood samples (normal and infected) using centrifuge machine (D-7200, Hitachi, Japan) at 3500 rpm for 20 min, and stored at -20^{0}C for subsequent studies.

2.2. Raman spectrum acquisition

Raman spectra from normal, as well as infected samples, were recorded on the same day after serum extraction by using a Raman system (Peak Seeker PRO-785). The spectrometer was attached with an inverted microscope (RSM-785, Agiltron, USA) for observing the sample. The laser source emitting laser beam at 785 nm were used for samples illumination. The microscope with the 10X objective was used focusing laser beam on the sample surface. For acquiring Raman spectra, samples were placed on the aluminum substrate- because of its low fluorescence background for the 785 nm excitation. From each sample ten different spectra were recorded (different position) in the spectral range from 400 to 1700 $cm^{-1,}$ laser power of 150 mW and signal collection time of 15 seconds.

Table 2
Confusion matrix obtained from the NNC algorithm based on the 18 peaks in the Raman spectra.

	HBV sample	Normal sample
HBV sample	119	01
Normal sample	01	169

Table 3
Performance evaluation metrics of the NNC algorithm.

Algorithm	S_n	S_p	*PPV*	*NPV*	*Acc*	*ROC Area*	*F measure*
NNC	0.992	0.994	0.992	0.994	0.993	0.99	0.992

2.3. Data pre- processing analysis

Raman spectra of biological samples typically contain significant noise. Similarly, the fluorescence background because of natural fluorophores also coupled with and distort the Raman signal. Specifically, the fluorescence signal is typically stronger in comparison to the weak signals in the Raman spectra. Therefore, data pre-processing was carried out before the spectral analyses for the possible differences in the two groups. Specifically, the spectra of the single sample were averaged and the average spectrum of each sera sample was then smoothed (with MATLAB 'sgoly' function), background subtracted (with MATLAB 'msbackadj' function), and normalized. Afterward, the spectrums from all HBV infected and normal samples were averaged out; the mean normalized spectrum of both groups (diseased and healthy samples) is depicted in Fig. 1. For clarity of the readers, the normalized mean spectrum of the diseased samples is shown in magenta color, whereas that of the normal samples is shown in green color. The details of the overall pre-processing have been previously described [10,17,18].

2.4. Neural network classifier (NNC)

Neural network classifier (NNC) is a widely used machine learning algorithm for classification problems, with the potential for both binary (i.e., yes/no decision) and multi-class (i.e., classify an entity into one of the several categories) classification. The fundamental working unit of NNC is called neuron, which has assigned a real value, modified by weight, and tuned via a non-linear activation function. A single layer of neurons receives part of the input variables. On similar grounds, multiple layers of neurons are constructed, where each layer passes on its results to the next layers. In this way, a neural network capable of learning the shape of any complex function is structured. NNC can efficiently handle high dimensionality problems and capable to understand the complex relations between variables. Specifically, the unique strength of NNC is its inherent potential to dynamically tune complex prediction functions with unparalleled precision [19].

3. Results and discussion

3.1. Spectral data analysis

All spectra from the diseased sera samples have been analyzed and compared with the healthy blood sera. The most significant intensity differences have been observed in Raman bands at 470, 520, 640, 680, 747, 765, 790, 830, 890, 910, 960, 1005, 1025, 1125, 1275, 1470, 1500, 1525, 1560 and 1580 cm^{-1}; these show the biochemical alteration that occurs in human blood in response to HBV infection. Thus, the present investigations can categorize the two classes of human blood sera for the identification of biochemical alterations occurring in the presence of HB viral infections.

The characteristic Raman peaks that appeared at 910 (C—C stretch of proline ring), 1070 and 1125 cm^{-1} (C—O—C asymmetric stretch) can be attributed to the glucose in the blood serum [20,21]. It can be inferred from Fig. 1 that the peak intensities have been increased in the HBV infected samples compared to the healthy one. The rise in peak intensities highlights the increased concentration of glucose in diseased patients, presumably due to the liver dysfunction to store glycogen leading to an increased level in the blood of HBV patients [22,23]. Therefore, it may be suggested that elevated glucose levels can be considered as a good biomarker for HBV diagnosis via Raman spectroscopy.

Raman peaks for bilirubin were observed at 1339, 1470 and 1611 cm^{-1}; the peak at 1470 cm-1 was due to the mixed stretching vibration of C—C and C–N and bending vibration of CH_3 groups, 1339 cm^{-1} was due to CH_2 bending vibration in CH_3 group, 1611 cm^{-1} was due to C═C stretching in five-membered ring [24]. The rise in peak intensity for infected samples indicated the increased level of bilirubin in the bloodstream. The abnormal level of bilirubin in the blood serum reflects the extent of hepatocellular damage and can be exploited to assess liver function and jaundice [25,26]. Peaks at Raman shift of 640, 675 and 830 cm^{-1} refer to the tyrosine, 747, 765 cm^{-1} were due to tryptophan, while 1005 and 1580 cm^{-1} were due to phenylalanine residues in serum albumin [27–29]. The respective rise in these peaks height indicate an elevated level of serum albumin in the infected blood sera. Albumin is a specific protein synthesized by the liver, which controls the balance of blood and carries the vital nutrients and hormones required in the body. The abnormal level of serum albumin reflects the dysfunction and inflammation of the liver in the HBV patients. Thus, the proposed approach can provide a promising tool for the quantification of albumin in the blood sera and an important marker for diagnosis and monitoring of HBV infection. Further, in the spectral region for Amide III (1200-1300 cm^{-1} due to the coupling of the C-N stretching and N-H bending), peak intensity at 1275 cm^{-1} specific for α-helical contents was increased as compared to 1230 and 1250 cm-1 for β-pleated structure [30]. It is well known that serum albumin have α-helical structure [31]. Thus, an enhancement of α- helix contents in the blood of infected samples may also indicate the increased concentration of serum albumin in HBV patients. Thus, the increasing intensity of this particular protein structure can be a possible biomarker that might contributes toward the classification of healthy and HBV infected individuals. On the other hand, the intensities of the peaks for the β-pleated structure are significantly decreased showing the decrease of particular Immunoglobin (IgG) protein in patients blood serum. The deviation from a normally expected Immunoglobin level serves as an indication of an Immunoglobin disorder as a result of liver infection. This is consistent with the previous studies that the elevated level of Immunoglobin in blood serum is the result of severe chronic HBV infection [32]. Thus, the Raman technique is a powerful tool which can provide a basis to generate an antibody profile of HBV in blood serum as well as diagnosis of Immunoglobin disorder due to HBV infection. The interferon (IFN-αA) is a protein that is naturally produced by lymphocytes in the immune response of HBV infections. A Raman peak of interferon showed the disulfide stretching band at 520 cm-1 [33], which has been increased in the infected samples. The increased intensity is indicative of high serum levels of interferon in HBV patients. As discussed earlier, according to the peaks observed for helical and beta structure in the region specific for Amide III, the concentration of helical structure proteins were increased. Thus, it can also be speculated that the increase in segments of helical structure in the infected samples may be due to increasing concentration of interferon in the response of severe viral attack. This is in accordance to the literature report that increases in helical structure as than the beta-structure in the amide III region, suggesting the secretion of interferon by lymphocytes as an immuning response against HBV infection [33]. Raman peak specifically appears at 1520 cm^{-1} which was assignable to the C═C stretching mode in beta-Carotene [34]. The increasing peak

intensity at 1516 cm^{-1} was due to the increasing concentration of beta-carotene in the HBV infected persons. This is in accordance with the previous reports that under an acute hepatic disorder, an excess of beta-carotene in the blood serum can cause hypercarotenemia or carotenes is or carotenoderma due to the impaired conversion of carotenoids to retinol, which is a common finding in the diagnosis of jaundice [34].

The Raman range (1640-1690 cm^{-1}) is associated with Amide I structure of a protein with a major contribution from C═O stretching vibration at 1650 cm^{-1} [25]. The decrease in intensity of peaks at 1650 and 1670 cm^{-1} in HBV infected samples compared to normal samples indicate the alteration of Amide I structure in blood serum due to pathogenic effect. Thus quantification and detection of Amide I can be an important biomarker for long term HBV diagnosis.

3.2. Model development

For machine assisted screening of the HBV infected samples, we developed an NNC based classification model. In the first phase, the spectra from both the healthy and HBV infected samples were thoroughly analyzed to identify prominent differences that can be subsequently exploited for the classification. A total of 18 peaks with prominent differences in the two spectra were identified, and their statistical significance was assessed by unpaired student t-test; a summary of the peak positions in the spectra, their differences, and the p-values along with the corresponding 95% confidence interval (CI) has been given in Table 1. It may be noted that the differences in 16 (out of 18) peaks were extremely significant with $p < 0.0001$. In the second phase, all the 18 Raman peaks were used in the NNC to classify the samples. Specifically, To construct the NNC for predicting the normal and HBV samples, the algorithm contained the input layer, hidden layer and output layer: the input layer contained 18 nodes corresponding to the 18 peaks/ attributes of the Raman spectra; the output layer contained 02 nodes corresponding to the two classes (i.e., normal versus HBV samples), while the hidden layer, which connects the input layer to the output layer, was composed of three layers with 5, 10 and 20 neurons, respectively. All of the neurons in the hidden layers used the standard sigmoid function($f(x) = (1 + e-x) - 1$) for learning/ training. For tuning the weights of the connections between the neurons, the value of the learning rate for the backpropagation was 0.3 while the momentum rate was set at 0.2. The resulting model was tested with the 10-fold cross-validation algorithm, followed by the prediction/ classification of the samples [35,36].

3.3. Model evaluation

The performance of the developed NNC model was assessed via the generated confusion matrix, as presented in Table 2. It may be noted that the correctly classified normal and HBV samples were 169/170 and 119/120, respectively. From the confusion matrix, different statistical terms such as accuracy (Acc), sensitivity (Sn), specificity (Sp), F-measure, positive predictive values (PPV) and negative predictive values (NPV) were calculated. From Table 3, it is clear that NNC provides 99.2%, 99.4% and 99.3% classification sensitivity, specificity, and accuracy, respectively. Further, the combinations of sensitivity and specificity were used for determining the area under the ROC curve, which provides a more direct metric for classification performance. The area under the ROC curve was 0.99. Moreover, positive and negative predictive values were found to be 99.2% and 99.4%, respectively.

4. Conclusions

This study demonstrate the applications of Raman spectroscopy for the analysis of HBV infected sera sample. In total 120 confirmed HBV diseased samples have been analyzed. Significant differences in the concentrations of important biomolecules such as glucose, albumin, cholesterol, triglycerides, phospholipids, alkaline phosphate, alanine aminotransferase, and aspartate transaminase have been observed in the HBV infected samples. These differences in the Raman spectra were used for machine-assisted classification of the two groups. The calculated evaluation metrics of the classification algorithm (i.e., neural network classifier) illustrated promise for the future clinical use of the proposed technique.

Declaration of Competing Interest

The authors declare that there is no conflicts of interest related to this article.

Acknowledgement

The author would like to thank all staff members at Agri-Biophotonics division, NILOP for assisting the present research work.

References

[1] WHO, Guidelines for the Prevention, Care and Treatment of Persons With Chronic Hepatitis B Infection, World Heal. Organ, Guidel, 2015, p. 166 (March).
[2] Muhammad Ali, Muhammad Idrees, Liaqat Ali, Abrar Hussain, Irshad Ur Rehman, Sana Saleem, Samia Afzal, S.B, Hepatitis B virus in Pakistan: a systematic review of prevalence, risk factors, awareness status and genotypes, Virol. J. 8 (102) (2011).
[3] M.-C. Chevrier, M. St-Louis, J. Perreault, B. Caron, C. Castilloux, J. Laroche, G. Delage, Detection and characterization of hepatitis B virus of anti-hepatitis B core antigen?reactive blood donors in Quebec with an in-house nucleic acid testing assay, Transfusion 47 (10) (2007) 1794–1802.
[4] A. Khabiri, M. Abolhassani, S. Aslani, H. Darabi, F. Bagheri, M.H. Alimohammadian, Compositional changes of PBL population in patients with chronic hepatitis B virus infection, Braz. J. Infect. Dis. 5 (6) (2001) 345–351.
[5] M. Krajden, J. Minor, L. Cork, L. Comanor, Multi-measurement method comparison of three commercial hepatitis B virus DNA quantification assays, J. Viral Hepat. 5 (6) (1998) 415–422.
[6] Yu-Huei Lin, Yi Wang, André Loua, Gwo-Jen Day, Yan Qiu, Elpidio Cesar B. Nadala Jr., Jean-Pierre Allain, Helen H. Lee, Evaluation of a new hepatitis B virus surface antigen rapid test with improved sensitivity, J. Clin. Microbiol. 46 (10) (2008) 3319–3324.
[7] P. Crow, J.S. Uff, J.A. Farmer, M.P. Wright, N. Stone, The use of Raman spectroscopy to identify and characterize transitional cell carcinoma in vitro, BJU Int. 93 (9) (2004) 1232–1236.
[8] S. Khan, R. Ullah, A. Khan, R. Ashraf, H. Ali, M. Bilal, M. Saleem, Analysis of hepatitis B virus infection in blood sera using Raman spectroscopy and machine learning, Photodiagn. Photodyn. Ther. 23 (2018).
[9] G.S. MohanSharma, Raman spectroscopy – basic principle, instrumentation and selected applications for the characterization of drugs of abuse, Egypt. J. Forensic Sci. 6 (3) (2016) 209–215.
[10] I. Ullah, I. Ahmad, H. Nisar, S. Khan, R. Ullah, R. Rashid, H. Mahmood, Computer assisted optical screening of human ovarian cancer using Raman spectroscopy, Photodiagn. Photodyn. Ther. 15 (2016).
[11] S. Khan, R. Ullah, M. Khurram, H. Ali, A. Mahmood, A. Khan, M. Ahmed, Evaluation of Raman spectroscopy in comparison to commonly performed dengue diagnostic tests, J. Biomed. Opt. 21 (9) (2016).
[12] Y.H. Ong, M. Lim, Q. Liu, Comparison of principal component analysis and biochemical component analysis in raman spectroscopy for the ciscrimination of apoptosis and necrosis in K562 leukemia cells, Opt. Express 20 (20) (2012) 22158–22171.
[13] C.J.C. Burges, A tutorial on support vector machine for pattern recognition, ata Min. Knowl. Discov. 2 (1998) 121–167.
[14] V. Vapnik, The Nature of Statistical Learning Theory, Springer, New York, 1995.
[15] M. Bilal, M. Saleem, Maria Bilal, M. Khurram, S. Khan, H.A. Rahat Ullah, M.A, Raman spectroscopy based discrimination of NS1 positive and negative dengue virus infected serum, Laser Phys. Lett. 13 (9) (2016) 095603.
[16] S.K. Teh, W. Zheng, K.Y. Ho, M. Teh, K.G. Yeoh, Z. Huang, Diagnostic potential of near-infrared Raman spectroscopy in the stomach: differentiating dysplasia from normal tissue, Br. J. Cancer 98 (2008) 457–465.
[17] S. Khan, R. Ullah, S. Shahzad, N. Anbreen, M. Bilal, Photodiagnosis and Photodynamic therapy analysis of tuberculosis disease through Raman spectroscopy and machine learning, Photodiagn. Photodyn. Ther. 24 (October) (2018) 286–291.
[18] S. Khan, R. Ullah, A. Khan, A. Sohail, N. Wahab, M. Bilal, M. Ahmed, Random forest-based evaluation of Raman spectroscopy for dengue fever analysis, Appl. Spectrosc. 71 (9) (2017).
[19] J.L. Patel, R.K. Goyal, Applications of artificial neural networks in medical science, Curr. Clin. Pharmacol. 2 (3) (2007) 217–226.
[20] Borges Rita de Cássia Fernandes, Ricardo Scarparo Navarro, Hector Enrique Giana, Fernanda Grubisich Tavares, Adriana Barrinha Fernandes, Landulfo Silveira Junior, Detecting alterations of glucose and lipid components in human serum by near-infrared Raman spectroscopy, Res. Biomed. Eng. 31 (2) (2015) 160–168.
[21] Jingwei Shao, Manman Lin, Yongqing Li, Xue Li, Junxian Liu, Jianpin Liang, H.Y, In vivo blood glucose quantification using Raman spectroscopy, PLoS One 7 (2012).

[22] Abdul Aziz Mustoi, Seema Bibi, Ahmed Shoaib, Bikha Ram Devrajani, S.A. Memon, G.A.Q, W.S, Metabolic investigation in hepatitis B patients with or without diabetes mellitus to determine the impact of anti-oxidant activity, World Appl. Sci. J. 15 (6) (2011) 765–771.
[23] Amna Ilyas, Sheikh Asrar Ahmad, Khalid Mehmood, Javed Tanveer Butt, Z.U.K, Study of relationship in glucose and serum glutamic pyruvate transaminase (SGPT) in blood serum of patients of Gujranwala District, Sci. Int. Lahore (Lahore) 26 (5) (2014) 2213–2216.
[24] T.S.S.K. Asha, Selective and sensitive sensing of free bilirubin in human serum using water-soluble polyfluorene as fluorescent probe, Macromolecules 48 (2015) 3449–3461.
[25] A. Rygula, K. Majzner, K.M. Marzec, A. Kaczor, M. Pilarczyk, M. Baranska, Raman spectroscopy of proteins: a review, J. Raman Spectrosc. 44 (8) (2013) 1061–1076.
[26] KOBOS, S.P.R, R, Jaundice in the adult patients, Am. Fam. Phys. 69 (9) (2004) 299–304.
[27] N.C. Dingari, G.L. Horowitz, J.W. Kang, R.R. Dasari, B.I, Raman spectroscopy provides a powerful diagnostic tool for accurate determination of albumin glycation, PLoS One 7 (2) (2012).
[28] A. Saha, Y.V, Structural changes of human serum albumin in response to a low concentration of heavy ions, J. Biophotonics 3 (10–11) (2010) 670–677.
[29] Achilles Dugaiczyk, SimonW. Law*, A.O.E.D, Nucleotide sequence and the encoded amino acids of human serum aibumin mRNA, Biochemistry 79 (1982) 71–75.
[30] E. Ryzhikova, O. Kazakov, L. Halamkova, D. Celmins, P. Malone, E. Molho, E.A. Zimmerman, I.K. Lednev, Raman spectroscopy of blood serum for Alzheimer's disease diagnostics: specificity relative to other types of dementia, J. Biophotonics 8 (7) (2015) 584–596.
[31] D.C. Carter, X.M. He, S.H. Munson, P.D. Twigg, K.M. Gernert, M.B. Broom, T.Y. Miller, Three-dimensional structure of human serum albumin, Science 244 (4909) (1989) 1195–1198.
[32] Riley C B, Mcclure J T, S.R.A. (2013) Identification of immunoglobulin (lg) disorders using fourier transform infrared spectroscopy. US Pat. No 8421019.
[33] R.W. Williams, Secondary structure of human leukocyte interferon from Raman spectroscopy, J. Biol. Chem. 260 (7) (1985) 3937–3940.
[34] Joke De Gelder, P.V. Kris De Gussem, L.M, Reference database of Raman spectra of biological molecules, J. Raman Spectrosc. 38 (2007) 1133–1147.
[35] A. Khan, A. Sohail, U. Zahoora, A.S. Qureshi, A Survey of the Recent Architectures of Deep Convolutional Neural Networks, (2019), pp. 1–62.
[36] A. Khan, A. Sohail, A. Ali, A New Channel Boosted Convolutional Neural Network using Transfer Learning, (2019), pp. 1–23.